MCB Accepted Manuscript Posted Online 1 February 2016
Mol. Cell. Biol. doi:10.1128/MCB.01021-15

MCB01021-15

De novo RNA synthesis by RNA-dependent RNA polymerase activity of TERT

Yoshiko Maida, Mami Yasukawa, Kenkichi Masutomi[#]

Division of Cancer Stem Cell, National Cancer Center Research Institute,

Tokyo, JAPAN

Running Head: *De novo* RNA synthesis by human TERT

#Address correspondence to Kenkichi Masutomi, M.D., Ph.D., kmasutom@ncc.go.jp

Y.M. and M.Y. contributed equally to this work.

Materials and Methods: 2069 words

Introduction, Results, and Discussion: 3077 words

Abstract

RNA-dependent RNA polymerase (RdRP) plays key roles in RNA silencing to generate double-stranded RNAs. In model organisms, such as *Caenorhabditis elegans* and *Neurospora crassa*, two types of small interfering RNAs (siRNAs), primary siRNAs and secondary siRNAs, are expressed, and RdRP produces secondary siRNAs *de novo* without using either Dicer or primers, while primary siRNAs are processed by Dicer. We reported that human TERT (telomerase reverse transcriptase) has RdRP activity and produces endogenous siRNAs in a Dicer-dependent manner. However, *de novo* synthesis of siRNAs by human TERT has not been elucidated. Here, we show that TERT RdRP generates short RNAs that were complementary to template RNAs and had 5'-triphosphorylated ends, which indicates *de novo* synthesis of the RNAs. In addition, we confirmed short RNA synthesis by TERT in several human carcinoma cell lines, and found that TERT protein levels were positively correlated with RdRP activity.

30 **Introduction**

31 TERT is known as the catalytic subunit of telomerase and is expressed at high levels
32 in cancer cells but only at low levels in normal human somatic cells. TERT elongates
33 telomeres by its RNA-dependent DNA polymerase (RdDP) activity using telomerase
34 RNA component (*TERC*) as the template. TERT and *TERC* assemble and form
35 telomerase; however, there is a population of TERT proteins that is not assembled into the
36 telomerase complex (1). Several lines of evidence indicate that TERT plays roles
37 independent of telomere maintenance; therefore, non-assembled TERT would be involved
38 in complexes other than telomerase.

39 RNA silencing is a sequence-specific gene-regulatory mechanism mediated by
40 double-stranded RNAs (dsRNAs). RdRP is a key player in RNA silencing, and the
41 polymerase is found in a variety of organisms including fungi, plants, and worms (2).
42 Although insects and mammals lack sequence homologues of cell-encoded RdRPs,
43 phylogenetic and structural analysis of TERT revealed that TERT is closely related to
44 RdRPs of RNA viruses as well as retroviral RdDPs (3). In fact, we found that TERT
45 generates dsRNA in a primer-dependent manner and works as an RdRP by a similar
46 mechanism to cell-encoded RdRPs (4, 5). Both viral RdRPs and cell-encoded RdRPs
47 transcribe single-stranded RNA (ssRNA) from template RNA not only in a
48 primer-dependent manner but also in a primer-independent manner. However, as a human
49 RdRP, primer-independent initiation of RNA synthesis by TERT remains to be elucidated.

50 To analyze the characteristics of the RdRP activity of human TERT, we established
51 an *in vitro* RdRP assay, in which we analyze RdRP activity of TERT immune complexes
52 immunoprecipitated from cell lysates with an anti-human TERT monoclonal antibody
53 (mAb) (IP-RdRP assay) (5). Here, we investigated the detailed characteristics of RNAs
54 processed through the IP-RdRP assay. The results indicate that TERT RdRP produces
55 short RNAs in a primer-independent manner. The relationship between TERT protein
56 levels and the RdRP activity of TERT was further confirmed in various carcinoma cell
57 lines.
58

Molecular and Cellular Biology

59 **Materials and Methods**

60 **Reagents**

61 The following reagents were used for the IP-RdRP assay: cOmplete EDTA-free protease
62 inhibitor cocktail (Roche), 3'-deoxyadenosine-5'-triphosphate (TriLink BioTechnologies),
63 3'-deoxycytidine-5'-triphosphate (TriLink BioTechnologies),
64 3'-deoxyguanosine-5'-triphosphate (TriLink BioTechnologies),
65 3'-deoxyuridine-5'-triphosphate (TriLink BioTechnologies), β-rubromycin (Enzo Life
66 Sciences), VX-222 (Selleckchem), and α-amanitin (Nacalai Tesque). Pefabloc SC
67 (AEBSF) (Roche) was used for the IP-TRAP assay.

68

69 **Antibodies**

70 Anti-human TERT mAbs (clones 10E9-2 and 2E4-2) were generated as reported
71 previously (5). Briefly, sense and antisense oligonucleotides corresponding to 304–460
72 amino acids of human TERT were cloned into plasmid pET-30a(+) (Novagen). A
73 recombinant carboxyl-terminal His-tagged TERT protein containing 157 amino acids
74 (position 304–460) was overexpressed in *E. coli* and purified with a nickel-agarose
75 column. Recombinant purified TERT was used as an immunogen to stimulate production
76 of anti-human TERT mAbs in mice using standard methodologies (5). A sequential
77 screening strategy was used to identify hybridomas producing anti-human TERT mAbs.

78 Primary antibodies used for immunoblotting were as follows: anti-phospho Histone

79 H3 (Ser10) polyclonal antibody (06-570, Millipore), anti-SNAIL polyclonal antibody
80 (ab17732, abcam), anti-human TWIST mouse mAb (clone Twist2C1a, Bio Matrix
81 Research), and anti-β-Actin mouse mAb (clone AC-15, Sigma-Aldrich). The following
82 antibodies were used for immunofluorescence analysis: anti-human TERT mAb (clone
83 2E4-2), anti-TRF2 polyclonal antibody (IMG-148A, Imgenex), anti-human Ki-67 antigen
84 mouse mAb (clone MIB-1, Dako), Alexa Fluor 488-conjugated donkey anti-mouse IgG
85 (H+L) (Life Technologies), and Alexa Fluor 568-conjugated donkey anti-goat IgG (H+L)
86 (Life Technologies).
87
88 **Peptide array**
89 A peptide array was performed as described previously (5). Seventy-five peptides derived
90 from a truncated version of human TERT (304–460 amino acids) were covalently bound
91 to a continuous cellulose membrane. The panel of peptides was then probed with an
92 anti-human TERT mAb, clone 2E4-2, and bound antibody was detected using the Pep
93 spot (Funakoshi) according to the manufacturer's protocol.
94
95 **Cell culture, mitotic cell synchronization, and transfection of siRNAs**
96 The human cervical carcinoma cell line HeLa, the SV40-transformed human embryonic
97 kidney cell line 293T, and the human hepatocellular carcinoma cell lines HepG2, HLE,
98 and HLF were cultured in DMEM supplemented with 10% heat-inactivated fetal bovine

99 serum (IFS). The human ovarian carcinoma cell lines were cultured as follows: RMG-I
100 was cultured in Ham's F12 medium supplemented with 10% IFS, TOV-21G was cultured
101 in MCDB105/Medium 199 (1:1) supplemented with 10% IFS, and PEO1 and PEO14
102 were cultured in RPMI-1640 medium supplemented with 10% IFS and 2 mM sodium
103 pyruvate (Gibco).

104 Mitotic cell synchronization was performed as described previously (5). Briefly,
105 cells were switched to medium containing 2.5 mM thymidine (Nacalai Tesque) and
106 incubated for 24 h. Six hours after release, cells were incubated in medium containing 0.1
107 μg/ml nocodazole (Invitrogen) for 14 h. After shake-off, mitotic cells were retrieved. For
108 suppression of TERT expression (Fig. 2C, 2D, and 2G), HeLa cells were transfected with
109 siRNAs using Lipofectamine 2000 (Invitrogen). After 48 h of incubation, cells were
110 treated with 0.1 μg/ml nocodazole (Invitrogen) for 16 h. 293T cells were transfected with
111 siRNAs using Lipofectamine 2000 (Invitrogen) twice, separated by 48 h, and cells were
112 harvested 24 h after the second transfection. The sequences used for the indicated
113 siRNAs were as follows (6): 5'-GUGUCUGUGCCCGGGAGAATT-3' and
114 5'-UUCUCCCGGGCACAGACACTT-3' for TERT siRNA #1, and 5'-
115 GCAUUGGAAUCAGACAGCATT-3' and 5'-UGCUGUCUGAUUCCAAUGCTT-3'
116 for TERT siRNA #2. MISSION siRNA Universal Negative Control #1 (Sigma-Aldrich
117 Japan) was used as a NC.
118

Molecular and Cellular Biology

119 **MTT assay**

120 Cells were seeded in 96-well dishes at 2.5×10^3 cells/well. After 96 h incubation, amount
121 of viable cells was quantified using the Cell Proliferation Kit I (MTT) (Roche) according
122 to the manufacturer's protocol.

123

124 **Immunofluorescence**

125 HeLa cells at 1.5×10^4 cells/well were seeded in 8-well CultureSlides (BD Falcon) 1 day
126 before transfection. TERT-specific siRNAs (TERT siRNA #1 and TERT siRNA #2) or
127 MISSION siRNA Universal Negative Control #1 (Sigma-Aldrich Japan) were transfected
128 twice, separated by 48 h, using Lipofectamine 2000 (Invitrogen). Cells were fixed for
129 immunofluorescence staining 48 h after the second transfection.

130 To synchronize HeLa cells in S phase, 1.4×10^4 of HeLa cells/well were seeded in
131 8-well CultureSlides (BD Falcon), and treated with 2 mM thymidine (Nacalai Tesque) for
132 14 h. Eleven hours after release, cells were incubated with 2 mM thymidine (Nacalai
133 Tesque) again for 14 h. Four hours after release, cells were fixed for immunofluorescence
134 analysis.

135 Immunofluorescence staining was performed as described previously (5). The cells
136 were observed under fluorescence microscopy (IX-81 without DSU, Olympus),
137 spinning-disk confocal microscopy (IX-81 with DSU, Olympus), or confocal microscopy
138 (FLUOVIEW FV10i, Olympus).

Molecular and Cellular Biology

Silkworm pupae overexpressing recombinant human TERT (rTERT)

Human TERT was expressed in the Silkworm-Baculovirus System produced by ProCube (Sysmex Corp., http://procube.sysmex.co.jp/eng/). The TERT gene was inserted into the transfer vector (Sysmex Corp.) based on the pUC19 vector for *Bombyx mori* nucleopolyhedrovirus (BmNPV). This transfer vector was co-transfected with baculovirus DNA (BmNPV CPd strain) (7) into a *Bombyx mori*-derived cell line (BmN) (8). After 7 days of incubation, the recombinant baculovirus was injected into the body of silkworm pupae, which were harvested 6 days after infection. In total, 5 ml of homogenization buffer (20 mM Tris-HCl (pH 7.4), 150 mM NaCl, 0.5% NP-40, 1 mM PMSF, 1 mM DTT, and phenylthiourea) was added per pupa, and homogenized using the homogenizer SH-IIM (ELMEX). The homogenates were immediately centrifuged at 100,000 × *g* at 4°C for 1 h. The supernatants containing TERT proteins were collected and used for the IP-IB and IP-RdRP assays.

Partial purification of rTERT

Twenty milligrams of silkworm lysate overexpressing rTERT was incubated with 40 µl of ANTI-FLAG M2-agarose (Sigma) overnight at 4°C. The beads were washed three times with Lysis buffer A (0.5% NP-40, 20 mM Tris-HCl (pH 7.4), and 150 mM NaCl), and eluted with FLAG peptides (Sigma). The elution was then incubated with 10 µg of an

159 anti-human TERT mAb (clone 10E9-2) and 40 µl of Pierce Protein A Plus Agarose
160 (Thermo Scientific) overnight at 4°C to obtain partially purified rTERT.
161
162 **IP-IB of TERT**
163 For human cell lines, 1×10^7 cells were lysed in 1 ml of Lysis buffer A. After sonication,
164 lysates were cleared of insoluble material by centrifugation at 21,000 × *g* at 4°C for 15
165 min. One milliliter of lysate was pre-absorbed with 40 µl of Pierce Protein A Plus
166 Agarose for 30 min at 4°C. Pre-absorbed lysate was mixed with 10 µg of an anti-human
167 TERT mAb (clone 10E9-2) and 40 µl of Pierce Protein A Plus Agarose, and incubated
168 overnight at 4°C. Immune complexes were washed three times with Lysis buffer A,
169 eluted in 2× SDS loading buffer (2% β-mercaptoethanol, 20% glycerol, 4% SDS, and 100
170 mM Tris-HCl (pH 6.8)), and then subjected to SDS-PAGE in 8% polyacrylamide gels. An
171 anti-human TERT mAb (clone 2E4-2) and MouseTrueBlot ULTRA (eBioscience) were
172 used for immunoblotting.
173 The amount of immunoprecipitated TERT proteins was estimated by SDS-PAGE
174 after Coomassie brilliant blue staining against bovine serum albumin (BSA). With 10 µg
175 of an anti-human TERT mAb (clone 10E9-2), 66 ng of rTERT was obtained from lysate
176 containing 20 mg of protein. ImageJ software was used to quantify the amount of
177 endogenous TERT proteins on the immunoblots.
178

Molecular and Cellular Biology

Synthetic RNAs

Synthetic RNAs used as templates for the IP-RdRP assay were as follows: RNA #1, 5'-GGGAUCAUGUGGGUCCUAUUACAUUUUAAACCCA-3'; RNA #2, 5'-GGGUUUAAAAUGUAAUAGGACCCACAUGAUCCCA-3'. The synthetic RNAs had hydroxyl groups at both the 5' and 3' ends. There are no identical sequences to either RNA #1 or RNA #2 in the human or *Bombyx mori* genome. A 3'-foldback structure was not predicted for RNA #1 or RNA #2 (9). Synthetic RNAs were reported as templates for RNA polymerization by Qβ replicase, a virus-encoded RdRP (9).

IP-RdRP assay

The IP-RdRP assay was performed as described previously (5). For IP followed by the RdRP assay of human cell lines, 1×10^7 cells were lysed in 1 ml of Lysis buffer A. After sonication, lysates were cleared of insoluble material by centrifugation at 21,000 × *g* at 4°C for 15 min. One milliliter of lysate, prepared from either cell cultures or silkworm pupae, was pre-absorbed with 40 µl of Pierce Protein A Plus Agarose for 30 min at 4°C. The pre-absorbed lysate was mixed with 10 µg of an anti-human TERT mAb (clone 10E9-2) and 40 µl of Pierce Protein A Plus Agarose, and incubated overnight at 4°C. Immune complexes were washed four times with 1× acetate buffer (10 mM HEPES-KOH (pH 7.8), 100 mM potassium acetate, and 4 mM $MgCl_2$) containing 10% glycerol, 0.1% Triton-X, and 0.06× cOmplete EDTA-free, and once with AGC solution (1× acetate

199 buffer containing 10% glycerol and 0.02% CHAPS) containing 2 mM $CaCl_2$. The bead
200 suspension was treated with 0.25 unit/µl MNase at 25°C for 15 min. Immunoprecipitates
201 were subsequently washed twice with AGC solution containing 3 mM EGTA and once
202 with 1× acetate buffer containing 0.02% CHAPS. Finally, 40 µl of reaction mixture was
203 prepared by combining 20 µl of the bead suspension, 6 µl of [α-^{32}P]UTP (3,000 Ci/mmol)
204 or [γ-^{32}P]ATP (3,000 Ci/mmol), and 25 ng/µl (final concentration) of RNA template and
205 supplements, and incubated at 32°C for 2 h. The final concentrations of ribonucleotides
206 were 1 mM ATP, 0.2 mM GTP, 10.5 µM UTP, and 0.2 mM CTP. The resulting products
207 were treated with Proteinase K to stop the reaction, purified several times with
208 phenol/chloroform until the white interface disappeared, and precipitated using ethanol.
209 For the UTP incorporation assay, RdRP products were treated with RNase I (2 U,
210 Promega) at 37°C for 2 h to digest ssRNAs, followed by Proteinase K treatment,
211 phenol/chloroform purification, and ethanol precipitation. The IP-RdRP products were
212 electrophoresed in a 10% polyacrylamide gel containing 7 M urea, and detected by
213 autoradiography. The amounts of products were compared by densitometry (ImageJ). The
214 amount of products generated with nocodazole-treated HeLa cells was used for
215 normalization.
216
217 **IP-TRAP assay**
218 For the TRAP assay using immunoprecipitated TERT, TERT protein was

Molecular and Cellular Biology

219 immunoprecipitated as described for the IP-RdRP assay without sonication. Immune
220 complexes were washed three times with Lysis buffer A, and then suspended in 35 µl of
221 TRAP lysis buffer (pH 7.5) (10 mM Tris-HCl, 1 mM $MgCl_2$, 1 mM EGTA, 0.5%
222 CHAPS, 10% glycerol, 100 µM Pefabloc SC, and 0.035% 2-mercaptoethanol). The
223 TRAP assay was performed with 2 µl of the suspension as described previously (5).
224
225 **RT-qPCR**
226 Cell lysate of nocodazole-treated HeLa cells was prepared as described for the IP-RdRP
227 assay, and total RNA was extracted from the lysate using Acid Phenol:$CHCl_3$ (Ambion)
228 followed by ethanol precipitation. TERT immune complex was immunoprecipitated from
229 the cell lysate, treated with MNase, and washed as described for the IP-RdRP assay. Total
230 RNA was then extracted from the TERT immune complex using TRIzol reagent
231 (invitrogen) according to the manufacturer's instructions. Reverse transcription was
232 performed using PrimeScript Reverse Transcriptase (TaKaRa) with pd$(N)_6$ Random
233 Hexamer (GE Healthcare). TaqMan Gene Expression assay (Hs03454202_s1, Applied
234 Biosystems) was used for quantitative PCR of *TERC*.
235
236 **Next-generation sequencing**
237 Ten batches of IP-RdRP products were pooled into one library for efficiency. The library
238 for deep sequencing of IP-RdRP products was constructed using NEBNext Multiplex

Molecular and Cellular Biology

239 Small RNA Library Prep Set for Illumina (New England BioLabs) essentially according
240 to the manufacturer's instructions. Libraries were sequenced using HiSeq 2000
241 (Illumina).

242 Ten batches of IP-RdRP products and the 3' SR Adaptor for Illumina were mixed
243 and denatured at 98°C for 1 min. Thereafter, 3' adaptor ligation was performed using the
244 denatured mixture, 3' Ligation Reaction Buffer, and 3' Ligation Enzyme Mix at 25°C for
245 1 h. Half the amount (0.5 µl) of SR RT Primer for Illumina was added to the mixture, and
246 then the mixture was denatured at 98°C for 1 min. To remove pyrophosphate from the 5'
247 ends of triphosphorylated RNA, the RNA mixture was incubated with RNA 5'
248 pyrophosphohydrolase (RppH) (New England BioLabs), and simultaneously incubated
249 with 5' SR Adaptor for Illumina, 5' Ligation Reaction Buffer, and 5' Ligase Enzyme Mix
250 for 5' adaptor ligation at 25°C for 1 h. After the rest of the SR RT Primer for Illumina was
251 added, the mixture was denatured at 70°C for 2 min, and then reverse transcription and
252 12 PCR cycles were performed according to the manufacturer's protocol. The PCR
253 products were purified by PAGE extraction, and six additional PCR cycles were
254 performed to obtain sufficient amounts of products for sequencing with HiSeq 2000.

255 Adapter sequences were identified and removed from sequencing reads for all
256 libraries. Sequences of 6 nt or longer were aligned to the RNA templates (RNA #1 and
257 RNA #2) used for the IP-RdRP assay using the blastn program of NCBI BLAST (version
258 2.2.28+).

Molecular and Cellular Biology

259

260 **Immunoblotting**

261 Immunoblot analysis was performed as described previously (5).

262

263 **Statistics**

264 Simple regression analyses were performed using Statcel3 software (OMS publishing). P

265 < 0.05 was considered significant.

266

Results

Endogenous TERT relates to RdRP activity as well as telomerase activity

We reported that TERT protein expression is enriched in mitotic phase in HeLa cells (5). To immunoprecipitate and detect endogenous TERT, we generated a series of anti-human TERT mAbs (clones 10E9-2 (5) and 2E4-2) (Figure 1) (5). We performed immunoprecipitation (IP) with clone 10E9-2 followed by immunoblotting with clone 2E4-2, and confirmed that TERT protein expression was enriched in HeLa cells treated with nocodazole in concordance with our previous report (5) (Fig. 2A). To investigate the detailed mode of action of RdRP activity by TERT, we modified the original IP-RdRP assay (5) using a chemically synthesized RNA of 34 nucleotides (nt) in length (RNA #1), which is more uniform than RNAs transcribed by T7 or SP6 RNA polymerases *in vitro*, as a template. Production of radioactive products was observed specifically in HeLa cells treated with nocodazole (Fig. 2B). The result suggests that RNA #1 would be utilized as a template for TERT RdRP activity, and that endogenous TERT detected by immunoblotting would be responsible for the product synthesis. To further validate the specificity of the antibodies, expression of endogenous TERT was suppressed by TERT-specific siRNAs in HeLa and 293T cells, and IP (clone 10E9-2) followed by immunoblotting (clone 2E4-2) (Fig. 2C) and the telomerase assay (Fig. 2D) was performed. Suppression of TERT expression by TERT-specific siRNAs eliminated the TERT protein signal in immunoblots (Fig. 2C) and telomerase activities (Fig. 2D) in both

Molecular and Cellular Biology

287 cell lines. The results demonstrate that endogenous TERT is immunoprecipitated (clone
288 10E9-2) and detected by clone 2E4-2. Specificity of clone 2E4-2 was further confirmed
289 by immunocytochemistry. Distinct nuclear staining, which was diminished by
290 TERT-specific siRNAs, was observed in HeLa cells stained with clone 2E4-2 (Fig. 2E).
291 In addition, the nuclear staining was colocalized with TRF2 in HeLa cells synchronized
292 into S phase (Fig. 2F). The immunofluorescent results again demonstrated specific
293 detection of endogenous TERT by clone 2E4-2. Furthermore, TERT-specific siRNAs
294 eliminated the IP-RdRP products (Fig. 2G), indicating that the radioactive products were
295 produced by TERT.
296
297 ***De novo* RNA synthesis by TERT RdRP**
298 To determine whether the products found in the IP-RdRP assay were indeed RNA
299 strands produced by polymerase activity, we investigated the requirement for
300 ribonucleotides in this assay. Exclusion of ribonucleotides abolished almost all the
301 products found in the IP-RdRP assay in HeLa cells treated with nocodazole (Fig. 3A).
302 Production was also inhibited by 3'-deoxyribonucleotide 5'-triphosphates (3'-dNTPs), a
303 type of chain-terminating ribonucleotides, in a dose-dependent manner (Fig. 3B). These
304 results indicate that all four types of ribonucleotide triphosphates are required to
305 synthesize the IP-RdRP products, and that the products are not generated by the terminal
306 transferase activity (10) but by the polymerase activity.

We next investigated whether RdRP activity of TERT is responsible for the RNA synthesis. First, we performed the IP-RdRP assay with either a telomerase inhibitor (β-rubromycin (11)) or DMSO (control). We previously confirmed that β-rubromycin inhibits telomerase activity (5), and, as shown in Figure 3C, RNA synthesis in this assay was remarkably inhibited by β-rubromycin. We next used VX-222, an RdRP inhibitor for NS5B of hepatitis C virus (HCV) (12). VX-222 fully inhibited RNA synthesis, while the same amount of VX-222 did not affect telomerase activity (Fig. 3D). These results strongly suggest that the TERT RdRP produces RNAs in the IP-RdRP assay. RNA polymerase (Pol) II is reportedly responsible for RdRP activity in *Saccharomyces cerevisiae* (13) and mouse (14); therefore, we excluded the possibility that Pol II is responsible for RNA production in this assay. For this purpose, we performed the IP-RdRP assay with α-amanitin, a well-characterized Pol II inhibitor. We found no effects of α-amanitin on RNA synthesis (Fig. 3E), which suggests that Pol II is not responsible for RNA synthesis in this assay. Taken together, we confirmed that human TERT synthesizes short RNAs through its RdRP activity.

We next investigated how short RNAs are synthesized by TERT RdRP. Since no primers were supplemented in our IP-RdRP assay and the 3'-foldback structure was not predicted for the template RNA #1 (9), short RNA synthesis in the IP-RdRP assay was assumed to be primer-independent (*de novo*). RNA species synthesized *de novo* carry characteristic 5'-triphosphate termini, while siRNAs cleaved by Dicer bear

Molecular and Cellular Biology

327 monophosphorylated 5' ends (15-17). To determine whether the short RNA products have
328 a 5'-triphosphate structure, we performed the IP-RdRP assay using [γ-^{32}P]ATP, which
329 specifically labels products with 5'-triphosphate termini (17). We found radioactive
330 IP-RdRP products specifically in HeLa cells treated with nocodazole (Fig. 3F). The
331 length of the products were identical to that observed in the IP-RdRP assay using
332 [α-^{32}P]UTP (Fig. 2B). This result indicates *de novo* synthesis of RNA species by TERT
333 RdRP in the assay.

334 As described above, there are two populations of TERT proteins, that assemble with
335 *TERC* and that do not (1). To examine whether *TERC* plays any roles in the *de novo* RNA
336 synthesis, we monitored *TERC* level in immune complexes prepared for the RdRP assay.
337 As shown in Figure 3G, we were unable to detect *TERC* in the TERT immune complexes
338 used for the RdRP assay, suggesting that TERT synthesized the RNAs independent of
339 *TERC*.

340 Some types of small silencing RNAs demonstrate characteristic bias in the
341 arrangement of residues as well as their length. To clarify the characteristics of the
342 primary structure of RNAs synthesized by TERT RdRP, we investigated these RNAs by
343 deep sequencing. We first analyzed IP-RdRP products of rTERT produced by silkworm
344 pupae (*Bombyx mori*) to elucidate the fundamental characteristics of TERT RdRP
345 products. We partially purified rTERT from silkworm pupae by IP with clone 10E9-2 and
346 performed the RdRP reaction (Fig. 4A). Intriguingly, rTERT demonstrated a remarkable

Molecular and Cellular Biology

347 preference for template RNAs in the RdRP reaction. Specifically, rTERT effectively
348 produced RNAs from template RNA #1, but not from template RNA #2 (Fig. 4A). rTERT
349 and template RNA #2 did not synthesize any RNA products; therefore, we used this
350 combination as a negative control (NC) and prepared two sets of IP-RdRP products for
351 deep sequencing: the products from RNA #1 (designated "rTERT-RNA #1") or RNA #2
352 (designated "rTERT-RNA #2") (Library 1, Table 1). In the library construction, we
353 treated the IP-RdRP products with RNA 5' pyrophosphohydrolase (RppH) (18) to enable
354 the ligation of 5' adapters to *de novo* synthesized RNAs, which have 5' triphosphate ends
355 (Fig. 4B). In total, 182 or 104 million sequences were obtained from each IP-RdRP
356 product (Table 1). Among them, sequences of 6 nt or longer were mapped onto the
357 template RNAs used in the IP-RdRP assay. The sequences used for mapping were
358 classified into five categories (Type A–D and Other, Table 1) according to the sequence
359 identity or similarity to either template RNA or its complementary strand. We specifically
360 focused on Type D sequences, which are completely complementary to a part of the
361 template RNA sequence. Because the silkworm genome does not contain any sequences
362 that are nearly identical to RNA #1 or RNA #2, Type D sequences found in the libraries
363 should be the anti-sense products of synthetic template RNAs. Consistent with the
364 IP-RdRP assay (Fig. 4A), the number of Type D sequences was 14-fold higher in
365 rTERT-RNA #1 than in rTERT-RNA #2 (251,672 vs. 17,945, Table 1). The length
366 distribution of Type D sequences traced the features of the IR-RdRP assay (Fig. 4A, 4C);

Molecular and Cellular Biology

367 there was a predominance of rTERT-RNA #1 against rTERT-RNA #2 with the highest
368 counts in ≈30 nt-products, indicating successful library construction for the IP-RdRP
369 products. We next investigated if there are any biases in residues at the 5' or 3' ends of
370 Type D sequences (> 20 nt) of rTERT-RNA #1. In total, 88.3% of Type D sequences in
371 rTERT-RNA #1 possessed purine residues at their 5' ends (A: 17.7% and G: 70.7%, Fig.
372 5A, 5B). As for 3' ends, 84.6% of Type D sequences terminated with C, and 60.0% of
373 them were placed at the 5' end of template RNA #1 (Fig. 5A, 5C).

374 We next sequenced IP-RdRP products prepared from HeLa cells treated with DMSO
375 or nocodazole, using RNA #1 as a template (DMSO-RNA #1 and nocodazole-RNA #1 of
376 Library 2, Table 1). The sequencing library was constructed with RppH treatment as
377 indicated in Figure 4B. It is noteworthy that nocodazole-RNA #1 demonstrated a
378 remarkably higher number of Type D sequences than DMSO-RNA #1 (4,287,182 vs.
379 118,320, Table 1). The results were consistent with the IP-RdRP assay using radioactivity
380 (Fig. 2B, 3F). The size distribution of Type D sequences indicated the specific production
381 of 20–30-nt RNAs by TERT, which was enriched in cells in mitotic phase (Fig. 4D). The
382 human genome does not contain consecutive sequences of 19 nt or longer that are
383 identical or complementary to template RNA #1. Therefore, we concluded that Type D
384 sequences of 19 nt or longer are not due to the contamination of cellular RNAs, but are
385 the products of the IP-RdRP assay. Specifically, the products are RNA strands newly
386 synthesized by TERT RdRP using RNA #1 as the template. We further investigated the 5'

Molecular and Cellular Biology

or 3' ends of Type D sequences (> 20 nt) of nocodazole-RNA #1. Nocodazole-RNA #1 demonstrated an apparently different distribution of 5' terminal residues compared to rTERT-RNA #1; 68.0% of sequences started with a purine residue (A: 33.9% and G: 34.1%), while 32.0% possessed a U at their 5' ends (Fig. 5A, 5B). In addition to 5' ends, the 3' ends of Type D sequences were more varied in nocodazole-RNA #1 than in rTERT-RNA #1 (Fig. 5A, 5C).

TERT protein levels correlate with RdRP activity

We found an association between TERT protein levels and RdRP activity as well as telomerase activity in both HeLa and 293T cells (Fig. 2). To clearly demonstrate the relationship between TERT protein levels and RdRP activity, the levels of rTERT protein (Fig. 6A) and its RdRP activity (Fig. 6B) were analyzed in various amounts of silkworm lysate. The results indicate a significant positive correlation between the levels of rTERT and RdRP activity (Fig. 6C).

Since we were able to calculate the rTERT level and RdRP activity *in vitro*, we monitored the levels of TERT and RdRP activities in human cancer cell lines. We first calculated that up to 1500 molecules of TERT were expressed per HeLa cell, consistent with a previous report (1). TERT protein levels and RdRP activities were then analyzed in human ovarian carcinoma (OC) and hepatocellular carcinoma (HCC) cell lines. TERT expression levels varied among the cell lines (Fig. 6D, 6G); TERT protein levels obtained

407 from each IP were high (≈30 ng) in HepG2 and HLE, but were low (<1 ng) in TOV-21G
408 and HLF. Short RNA products of the IP-RdRP assay were found in OC and HCC cell
409 lines with moderate to high levels of TERT proteins (RMG-I, PEO1, PEO14, HepG2, and
410 HLE), while these products were almost absent in cell lines with low levels of TERT
411 (TOV-21G and HLF) (Fig. 6E). Telomerase activity was also comparable to RdRP
412 products; moderate to high levels of telomerase activity was detected in the cell lines with
413 RdRP products, and telomerase activity was very weak in the cell lines with little product
414 (Fig. 6F). The association between the levels of TERT proteins and RdRP products was in
415 agreement with the results obtained using HeLa cells treated with or without nocodazole
416 (Fig. 2A, 2B) as well as TERT suppression in both HeLa and 293T cells (Fig. 2C, 2D,
417 and 2G). Simple regression analysis revealed a positive correlation between levels of
418 endogenous TERT protein and RdRP activity (Fig. 6G). Taken together, these data
419 suggest that TERT protein levels are the rate-limiting factor of the RdRP activity.
420 We next examined characteristics of OC and HCC cell lines and TERT protein
421 /RdRP activity. We analyzed cell proliferation as gauged by cell growth (Fig. 6H), Ki-67
422 expression (Fig. 6I), and phospho-histone H3 (Ser10) levels (Fig. 6J) and metastatic
423 potentialities as gauged by expression level of epithelial-mesenchymal transition
424 (EMT)-related genes, such as SNAIL and TWIST1 (Fig. 6J). In these analyses, however,
425 we were unable to find out any conclusive relationships between TERT protein/RdRP
426 activity and cell proliferation or EMT-related gene expression.
427

Molecular and Cellular Biology

Discussion

RNA polymerization by telomerase was first described in *Tetrahymena* (19). Using the telomerase RNA components as template, *Tetrahymena* telomerase incorporated rGTP as well as dTTP to synthesize the chimeric product of [d(TT)r(GGGG)]n that was complementary to the template RNA. DNA elongation from RNA primer by *Tetrahymena* telomerase was also described in the same study (19), that indicated competency of the enzyme to bind dsRNAs. We have reported RNA primer requirement to synthesize dsRNA by human TERT through its RdRP activity (4). A fundamental difference between DNA and RNA polymerases is that RNA polymerases do not necessarily require primers to initiate nucleotide polymerization while DNA polymerases do. Indeed, both viral RdRPs and cell-encoded RdRPs initiate complementary RNA strand synthesis in either a primer-dependent or -independent manner (15, 16, 20, 21). Biological significance of primer-independent RNA polymerization by these RdRPs has been demonstrated. For example, RdRPs of RNA viruses use primer-independent (*de novo*) initiation mechanism for complete replication of their genomes (22, 23). RdRPs in *Caenorhabditis elegans* (*C. elegans*), specifically RRF-1 and EGO-1, engage *de novo* synthesis of 22-nt RNAs, which are known as secondary siRNAs, and contribute to amplify RNA silencing signals triggered by primary siRNAs (15, 16). In this study, we confirmed *de novo* RNA synthesis by RdRP activity of TERT, suggesting that TERT shares common features with viral and cell-encoded RdRPs in initiation step of RNA polymerization, and there may be

Molecular and Cellular Biology

unknown biological processes mediated by the *de novo* synthesized RNAs in human cells expressing TERT.

Functional small RNAs are often classified based on their length and nucleotide biases. For instance, *C. elegans* expresses three different classes of small RNAs, 26G-, 22G-, and 21U-RNAs (24, 25); the names of these RNAs reflect the size of each RNA and the preference for G or U residues at their 5' ends. Among these RNA classes, 22G-RNAs are secondary siRNAs synthesized *de novo* by RdRP (25, 26). In addition to 22G-RNA in *C. elegans*, viral RdRPs usually start *de novo* RNA synthesis with purine residues (22, 23). Particularly, G is the most universal initiation nucleotide, and complementary C at or near the 3' terminus of RNA template is recognized as the initiation site by viral RdRPs (21). RNA templates used in this study have 5'-CCCA-3' sequence at their 3' end, and we found that 70.7% of complementary RNA strand synthesis in rTERT-RNA #1 was initiated with G, most of which were mapped on the 5'-CCCA-3' sequence. This result indicates that TERT preserves the common property of RdRPs in priming *de novo* RNA synthesis.

The preference for 5' purine residues in nocodazole-RNA #1 was, however, lower than that reported for RdRP of *C. elegans* (RRF-1). In sequencing analysis of the RNA products of RRF-1, more than 90% of the products possessed a purine residue at their 5' ends (17). The ratio of 5' purine in nocodazole-RNA #1 (68.0%) was also lower than that in rTERT-RNA #1 (88.3%). Conversely, stringency in the initiation nucleotide would be

Molecular and Cellular Biology

468 relaxed in endogenous TERT (nocodazole-RNA #1) compered to rTERT (rTERT-RNA
469 #1). These results imply that there is a mechanism(s) that enhances the flexibility of *do*
470 *novo* RNA synthesis by endogenous TERT and thereby increases the diversity of RNA
471 species produced in human cells.

472 Increased *TERT* expression and subsequent telomerase activation is a common
473 feature of human cancers. A recent study by Borah *et al*. demonstrated that both TERT
474 mRNA and protein levels correlate strongly with telomerase activity in urothelial
475 carcinoma cell lines (27). As a counterpart to research focusing on telomerase activity, we
476 analyzed protein levels and RdRP activity of endogenous TERT in OC and HCC in this
477 study, and found that TERT protein levels were positively correlated with RdRP activity.
478 It would be important to revisit why most of human cancers express TERT based on the
479 understanding that TERT is a multifunctional protein; not only telomere maintenance by
480 telomerase activity, but also RNA regulation by the RdRP activity would be crucial for
481 human carcinogenesis.

482 In the past decade, many different types of functional small RNAs have been
483 reported, and we now know that these RNA-related pathways regulate diverse
484 physiological and pathological processes. As is found in plants and worms, *de novo*
485 synthesis of RNAs by TERT RdRP might shed further light on the mechanism underlying
486 RNA silencing in human cells, especially malignant cells. Given that the *TERT*
487 expression level is critical for the carcinogenic process of various cancers (27-30), in

Molecular and Cellular Biology

488 addition to authentic telomerase activity, the RdRP activity of TERT might be a novel

489 promising molecular target for cancer treatment.

Molecular and Cellular Biology

Funding Information

This work was supported in part by the Project for Development of Innovative Research on Cancer Therapeutics (P-DIRECT), Japan Agency for Medical Research and Development (Kenkichi Masutomi), the Takeda Science Foundation (Yoshiko Maida), and a Research Grant of the Princess Takamatsu Cancer Research Fund 13-24520 (Yoshiko Maida). The funders had no role in study design, data collection and interpretation, or the decision to submit the work for publication.

498 **References**

499 1. **Xi L, Cech TR.** 2014. Inventory of telomerase components in human cells reveals
500 multiple subpopulations of hTR and hTERT. Nucleic Acids Res **42:**8565-8577.
501 2. **Siomi H, Siomi MC.** 2009. On the road to reading the RNA-interference code.
502 Nature **457:**396-404.
503 3. **Nakamura TM, Morin GB, Chapman KB, Weinrich SL, Andrews WH, Lingner**
504 **J, Harley CB, Cech TR.** 1997. Telomerase catalytic subunit homologs from fission
505 yeast and human. Science **277:**955-959.
506 4. **Maida Y, Yasukawa M, Furuuchi M, Lassmann T, Possemato R, Okamoto N,**
507 **Kasim V, Hayashizaki Y, Hahn WC, Masutomi K.** 2009. An RNA-dependent
508 RNA polymerase formed by TERT and the RMRP RNA. Nature **461:**230-235.
509 5. **Maida Y, Yasukawa M, Okamoto N, Ohka S, Kinoshita K, Totoki Y, Ito TK,**
510 **Minamino T, Nakamura H, Yamaguchi S, Shibata T, Masutomi K.** 2014.
511 Involvement of telomerase reverse transcriptase in heterochromatin maintenance.
512 Mol Cell Biol **34:**1576-1593.
513 6. **Okamoto N, Yasukawa M, Nguyen C, Kasim V, Maida Y, Possemato R, Shibata**
514 **T, Ligon KL, Fukami K, Hahn WC, Masutomi K.** 2011. Maintenance of tumor
515 initiating cells of defined genetic composition by nucleostemin. Proc Natl Acad Sci
516 U S A **108:**20388-20393.
517 7. **Suzuki T, Kanaya T, Okazaki H, Ogawa K, Usami A, Watanabe H,**

518 **Kadono-Okuda K, Yamakawa M, Sato H, Mori H, Takahashi S, Oda K.** 1997.
519 Efficient protein production using a Bombyx mori nuclear polyhedrosis virus lacking
520 the cysteine proteinase gene. J Gen Virol **78** (Pt 12):3073-3080.

521 8. **Maeda S, Mitsuhashi J.** 1989. Gene transfer vectors of a baculovirus Bombyx mori
522 and their use for expression of foreign genes in insect cells, p 167-181, Invertebrate
523 Cell System Applications. CRC Press, Boca Raton, Fla.

524 9. **Zamora H, Luce R, Biebricher CK.** 1995. Design of artificial short-chained RNA
525 species that are replicated by Q beta replicase. Biochemistry **34:**1261-1266.

526 10. **Lue NF, Bosoy D, Moriarty TJ, Autexier C, Altman B, Leng S.** 2005. Telomerase
527 can act as a template- and RNA-independent terminal transferase. Proc Natl Acad
528 Sci U S A **102:**9778-9783.

529 11. **Mizushina Y, Takeuchi T, Sugawara F, Yoshida H.** 2012. Anti-cancer targeting
530 telomerase inhibitors: beta-rubromycin and oleic acid. Mini Rev Med Chem
531 **12:**1135-1143.

532 12. **Yi G, Deval J, Fan B, Cai H, Soulard C, Ranjith-Kumar CT, Smith DB, Blatt L,**
533 **Beigelman L, Kao CC.** 2012. Biochemical study of the comparative inhibition of
534 hepatitis C virus RNA polymerase by VX-222 and filibuvir. Antimicrob Agents
535 Chemother **56:**830-837.

536 13. **Lehmann E, Brueckner F, Cramer P.** 2007. Molecular basis of RNA-dependent
537 RNA polymerase II activity. Nature **450:**445-449.

Molecular and Cellular Biology

538 14. **Wagner SD, Yakovchuk P, Gilman B, Ponicsan SL, Drullinger LF, Kugel JF,**
539 **Goodrich JA.** 2013. RNA polymerase II acts as an RNA-dependent RNA
540 polymerase to extend and destabilize a non-coding RNA. EMBO J **32:**781-790.
541 15. **Sijen T, Steiner FA, Thijssen KL, Plasterk RH.** 2007. Secondary siRNAs result
542 from unprimed RNA synthesis and form a distinct class. Science **315:**244-247.
543 16. **Pak J, Fire A.** 2007. Distinct populations of primary and secondary effectors during
544 RNAi in C. elegans. Science **315:**241-244.
545 17. **Aoki K, Moriguchi H, Yoshioka T, Okawa K, Tabara H.** 2007. In vitro analyses
546 of the production and activity of secondary small interfering RNAs in C. elegans.
547 EMBO J **26:**5007-5019.
548 18. **Deana A, Celesnik H, Belasco JG.** 2008. The bacterial enzyme RppH triggers
549 messenger RNA degradation by 5' pyrophosphate removal. Nature **451:**355-358.
550 19. **Collins K, Greider CW.** 1995. Utilization of ribonucleotides and RNA primers by
551 Tetrahymena telomerase. EMBO J **14:**5422-5432.
552 20. **Makeyev EV, Bamford DH.** 2002. Cellular RNA-dependent RNA polymerase
553 involved in posttranscriptional gene silencing has two distinct activity modes. Mol
554 Cell **10:**1417-1427.
555 21. **van Dijk AA, Makeyev EV, Bamford DH.** 2004. Initiation of viral RNA-dependent
556 RNA polymerization. J Gen Virol **85:**1077-1093.
557 22. **Kao CC, Singh P, Ecker DJ.** 2001. De novo initiation of viral RNA-dependent

558 RNA synthesis. Virology **287:**251-260.

559 23. **Luo G, Hamatake RK, Mathis DM, Racela J, Rigat KL, Lemm J, Colonno RJ.**
560 2000. De novo initiation of RNA synthesis by the RNA-dependent RNA polymerase
561 (NS5B) of hepatitis C virus. J Virol **74:**851-863.

562 24. **Kamminga LM, van Wolfswinkel JC, Luteijn MJ, Kaaij LJ, Bagijn MP,**
563 **Sapetschnig A, Miska EA, Berezikov E, Ketting RF.** 2012. Differential impact of
564 the HEN1 homolog HENN-1 on 21U and 26G RNAs in the germline of
565 Caenorhabditis elegans. PLoS Genet **8:**e1002702.

566 25. **Claycomb JM, Batista PJ, Pang KM, Gu W, Vasale JJ, van Wolfswinkel JC,**
567 **Chaves DA, Shirayama M, Mitani S, Ketting RF, Conte D, Jr., Mello CC.** 2009.
568 The Argonaute CSR-1 and its 22G-RNA cofactors are required for holocentric
569 chromosome segregation. Cell **139:**123-134.

570 26. **Gu W, Shirayama M, Conte D, Jr., Vasale J, Batista PJ, Claycomb JM, Moresco**
571 **JJ, Youngman EM, Keys J, Stoltz MJ, Chen CC, Chaves DA, Duan S, Kasschau**
572 **KD, Fahlgren N, Yates JR, 3rd, Mitani S, Carrington JC, Mello CC.** 2009.
573 Distinct argonaute-mediated 22G-RNA pathways direct genome surveillance in the
574 C. elegans germline. Mol Cell **36:**231-244.

575 27. **Borah S, Xi L, Zaug AJ, Powell NM, Dancik GM, Cohen SB, Costello JC,**
576 **Theodorescu D, Cech TR.** 2015. TERT promoter mutations and telomerase
577 reactivation in urothelial cancer. Science **347:**1006-1010.

578 28. **Huang FW, Hodis E, Xu MJ, Kryukov GV, Chin L, Garraway LA.** 2013. Highly
579 recurrent TERT promoter mutations in human melanoma. Science **339:**957-959.
580 29. **Totoki Y, Tatsuno K, Covington KR, Ueda H, Creighton CJ, Kato M, Tsuji S,**
581 **Donehower LA, Slagle BL, Nakamura H, Yamamoto S, Shinbrot E, Hama N,**
582 **Lehmkuhl M, Hosoda F, Arai Y, Walker K, Dahdouli M, Gotoh K, Nagae G,**
583 **Gingras MC, Muzny DM, Ojima H, Shimada K, Midorikawa Y, Goss JA,**
584 **Cotton R, Hayashi A, Shibahara J, Ishikawa S, Guiteau J, Tanaka M,**
585 **Urushidate T, Ohashi S, Okada N, Doddapaneni H, Wang M, Zhu Y, Dinh H,**
586 **Okusaka T, Kokudo N, Kosuge T, Takayama T, Fukayama M, Gibbs RA,**
587 **Wheeler DA, Aburatani H, Shibata T.** 2014. Trans-ancestry mutational landscape
588 of hepatocellular carcinoma genomes. Nat Genet **46:**1267-1273.
589 30. **Peifer M, Hertwig F, Roels F, Dreidax D, Gartlgruber M, Menon R, Kramer A,**
590 **Roncaioli JL, Sand F, Heuckmann JM, Ikram F, Schmidt R, Ackermann S,**
591 **Engesser A, Kahlert Y, Vogel W, Altmuller J, Nurnberg P, Thierry-Mieg J,**
592 **Thierry-Mieg D, Mariappan A, Heynck S, Mariotti E, Henrich KO, Gloeckner**
593 **C, Bosco G, Leuschner I, Schweiger MR, Savelyeva L, Watkins SC, Shao C,**
594 **Bell E, Hofer T, Achter V, Lang U, Theissen J, Volland R, Saadati M, Eggert A,**
595 **de Wilde B, Berthold F, Peng Z, Zhao C, Shi L, Ortmann M, Buttner R, Perner**
596 **S, Hero B, Schramm A, Schulte JH, Herrmann C, O'Sullivan RJ, Westermann**
597 **F, Thomas RK, Fischer M.** 2015. Telomerase activation by genomic

Molecular and Cellular Biology

598 rearrangements in high-risk neuroblastoma. Nature **526:**700-704.

599

Molecular and Cellular Biology

600 **Figure legends**

601 **Figure 1. Confirmation of the specificity of anti-human TERT mAbs**

602 (**A**) Peptides used to map the TERT epitope (5). The truncated version of human TERT
603 (304–460 amino acids) used to generate mAbs was divided in 75 peptides.

604 (**B**) Epitope mapping for clone 2E4-2 by the peptide array. Numbers indicate specific
605 peptides.

606

607 **Figure 2. Enzymatic activities of endogenous TERT**

608 Endogenous TERT was immunoprecipitated from HeLa and 293T cells with an
609 anti-human TERT mAb (clone 10E9-2). An anti-human TERT mAb (clone 2E4-2) was
610 used for immunoblotting.

611 (**A**) IP-IB of endogenous TERT. HeLa cells were treated with nocodazole (manipulated)
612 or DMSO (unmanipulated). The signals ≈52 kDa indicate heavy chains of IgG.

613 (**B**) IP-RdRP assay using HeLa cells treated with nocodazole or DMSO. [α-^{32}P]UTP and
614 synthetic RNA (RNA #1) were used.

615 (**C, D**) HeLa cells treated with nocodazole or 293T cells were transfected with
616 TERT-specific (TERT siRNA #1 and TERT siRNA #2) or NC siRNA.

617 (**C**) IP-IB of endogenous TERT. The signals ≈52 kDa indicate heavy chains of IgG.

618 (**D**) IP followed by the telomeric repeat amplification protocol (TRAP) (IP-TRAP) assay.
619 IC, internal control.

620 (**E**) Immunofluorescence of HeLa cells transfected with TERT-specific (TERT siRNA #1
621 and TERT siRNA #2) or NC siRNA. TERT was immunostained with an anti-human
622 TERT mAb (clone 2E4-2).
623 (**F**) Colocalization of endogenous TERT with TRF2 in HeLa cells. An anti-human TERT
624 mAb (clone 2E4-2) and an anti-TRF2 antibody were used for staining.
625 (**G**) IP-RdRP assay using [α-^{32}P]UTP and synthetic RNA (RNA #1). HeLa and 293T cells
626 were prepared in the same way as (**C**) and (**D**).
627
628 **Figure 3. TERT RdRP generates short RNA strands *de novo***
629 The IP-RdRP assay was performed with HeLa cells treated with nocodazole using
630 [α-^{32}P]UTP (**A**–**E**) or [γ-^{32}P]ATP (**F**). Synthetic RNA (RNA #1) was used as a template.
631 (**A**) IP-RdRP assay. All four types of ribonucleotides (Control) or rUTP alone (rNTP(-))
632 was added.
633 (**B**) Supplemented ribonucleotides in the IP-RdRP assay were replaced by 3'-dNTPs at
634 the indicated concentrations.
635 (**C**) Suppression of RNA synthesis by a telomerase inhibitor. β-rubromycin was used for
636 the IP-RdRP assay.
637 (**D**) Suppression of RNA synthesis, but not telomerase activity, by an RdRP inhibitor.
638 HeLa cells treated with nocodazole were used for the IP-RdRP and IP-TRAP assays.
639 VX-222 (100 μM) was used. IC, internal control.

640 (**E**) No effects of α-amanitin on RNA synthesis. α-amanitin at the indicated
641 concentrations was used for the IP-RdRP assay.
642 (**F**) The IP-RdRP assay using [γ-^{32}P]ATP. HeLa cells treated with nocodazole or DMSO
643 were used.
644 (**G**) RT-qPCR of *TERC* in HeLa cells treated with nocodazole. Total RNA was extracted
645 from cell lysate (Input, 0.13%) or TERT immune complexes prepared for the RdRP assay
646 (IP, 2%). RT (-) denotes that reverse transcriptase reaction was performed without reverse
647 transcriptase.
648
649 **Figure 4. Properties of short RNAs synthesized by TERT RdRP**
650 (**A**) The IP-RdRP assay using the lysate of silkworm pupae overexpressing rTERT, an
651 anti-human TERT mAb (clone 10E9-2), and [α-^{32}P]UTP. Synthetic RNAs (RNA #1 and
652 RNA #2) were used as templates. The IP-RdRP assay without template RNA was
653 performed as a NC (Control).
654 (**B**) Scheme for the preparation of a small RNA library for deep sequencing analysis of
655 IP-RdRP products. RppH was used to convert 5' ends of triphosphate to monophosphate.
656 The library could be successfully constructed from 5' triphosphorylated RNAs with
657 RppH treatment.
658 (**C**) Length distribution of Type D sequences in rTERT-RNA #1 (black bars) and
659 rTERT-RNA #2 (white bars). IP-RdRP products of rTERT were analyzed by deep

660 sequencing.

661 (**D**) Length distribution of Type D sequences in DMSO-RNA #1 (white bars) and
662 nocodazole-RNA #1 (black bars). Short RNA products in the IP-RdRP assay using HeLa
663 cells were analyzed by deep sequencing.

664

665 **Figure 5. Start and end positions of short RNAs synthesized by TERT RdRP**

666 Deep sequencing analysis of short RNA products in the IP-RdRP assay.

667 (**A**) Mapping of Type D sequences in rTERT-RNA #1 (left panel) and nocodazole-RNA
668 #1 (right panel). The most frequent sequences in each sequence length are presented.
669 Counts of each sequence are listed.

670 (**B**, **C**) 5' end (**B**) and 3' end (**C**) of Type D sequences obtained from rTERT-RNA #1 and
671 nocodazole-RNA #1 are indicated.

672

673 **Figure 6. TERT protein levels are correlated with RdRP activity**

674 (**A**–**C**) Positive correlation between the levels of rTERT and RdRP activity.

675 (**A**) IP-IB and (**B**) IP-RdRP assays were performed with the indicated amount of
676 silkworm lysate overexpressing rTERT. The amount of rTERT immunoprecipitated from
677 each lysate was calculated by comparing the signals obtained by IP-IB (**A**).

678 (**C**) Protein levels versus relative RdRP activity for rTERT. Relative RdRP activity was
679 plotted in arbitrary units.

680 (**D**–**G**) Expression levels and enzymatic activity of TERT protein in OC and HCC cell
681 lines were analyzed.
682 (**D**) IP-IB of OC and HCC cell lines. The signals ≈52 kDa indicate heavy chains of IgG.
683 (**E**) IP-RdRP assays of OC and HCC cell lines.
684 (**F**) IP-TRAP assays of OC and HCC cell lines. IC, internal control.
685 (**G**) TERT protein versus relative RdRP activity for each of the OC and HCC cell lines.
686 Mean values from two independent experiments were plotted.
687 (**H**) Cell growth of OC and HCC cell lines was analyzed by MTT assay.
688 (**I**) Ki-67-positive ratios were calculated based on immunofluorescence analysis.
689 Representative images are shown.
690 (**J**) Immunoblot analysis of OC and HCC cell lines.

Molecular and Cellular Biology

691 **Table 1.** Classification of sequences obtained by deep sequencing.

692

	Library 1		Library 2	
Type	rTERT-RNA #1	rTERT-RNA #2	DMSO-RNA #1	nocodazole-RNA #1
A*	1,159,555	14,776	31,355	8,804
B †	39,340,949	43,335,025	93,651,643	54,932,629
C ‡	0	0	0	0
D §	251,672	17,945	118,320	4,287,182
Other	141,370,214	60,833,729	68,867,660	102,515,449
Total reads	182,122,390	104,201,475	162,668,978	161,744,064

693 The RNA products of the IP-RdRP assay were analysed by deep sequencing. The
694 obtained sequences (> 6 nt) were mapped to the template sequence and classified into
695 five categories (Type A-D and Other) as indicated. Total reads indicate number of
696 sequences used for mapping.

697 *Type A: Completely identical to template RNA

698 †Type B: Completely identical to a part of the sequence of template RNA

699 ‡Type C: Completely complementary to template RNA

700 §Type D: Completely complementary to a part of the sequence of template RNA

Molecular and Cellular Biology

A

Peptide No.	a.a. No.	Sequence											
1	304	HAGPPSTSRP	21	344	SFLLSSLRPS	41	384	QRYWQMRPLF	61	424	GVCAREKPQG
2	306	GPPSTSRPPR	22	346	LLSSLRPSLT	42	386	YWQMRPLFLE	62	426	CAREKPQGSV
3	308	PSTSRPPRPW	23	348	SSLRPSLTGA	43	388	QMRPLFLELL	63	428	REKPQGSVAA
4	310	TSRPPRPWDT	24	350	LRPSLTGARR	44	390	RPLFLELLGN	64	430	KPQGSVAAPE
5	312	RPPRPWDTPC	25	352	PSLTGARRLV	45	392	LFLELLGNHA	65	432	QGSVAAPEEE
6	314	PRPWDTPCPP	26	354	LTGARRLVET	46	394	LELLGNHAQC	66	434	SVAAPEEEDT
7	316	PWDTPCPPVY	27	356	GARRLVETIF	47	396	LLGNHAQCPY	67	436	AAPEEEDTDP
8	318	DTPCPPVYAE	28	358	RRLVETIFLG	48	398	GNHAQCPYGV	68	438	PEEEDTDPRR
9	320	PCPPVYAETK	29	360	LVETIFLGSR	49	400	HAQCPYGVLL	69	440	EEDTDPRRLV
10	322	PPVYAETKHF	30	362	ETIFLGSRPW	50	402	QCPYGVLLKT	70	442	DTDPRRLVQL
11	324	VYAETKHFLY	31	364	IFLGSRPWMP	51	404	PYGVLLKTHC	71	444	DPRRLVQLLR
12	326	AETKHFLYSS	32	366	LGSRPWMPGT	52	406	GVLLKTHCPL	72	446	RRLVQLLRQH
13	328	TKHFLYSSGD	33	368	SRPWMPGTPR	53	408	LLKTHCPLRA	73	448	LVQLLRQHSS
14	330	HFLYSSGDKE	34	370	PWMPGTPRRL	54	410	KTHCPLRAAV	74	450	QLLRQHSSPW
15	332	LYSSGDKEQL	35	372	MPGTPRRLPR	55	412	HCPLRAAVTP	75	452	LRQHSSPWQ
16	334	SSGDKEQLRP	36	374	GTPRRLPRLP	56	414	PLRAAVTPAA			
17	336	GDKEQLRPSF	37	376	PRRLPRLPQR	57	416	RAAVTPAAGV			
18	338	KEQLRPSFLL	38	378	RLPRLPQRYW	58	418	AVTPAAGVCA			
19	340	QLRPSFLLSS	39	380	PRLPQRYWQM	59	420	TPAAGVCARE			
20	342	RPSFLLSSLR	40	382	LPQRYWQMRP	60	422	AAGVCAREKP			

B

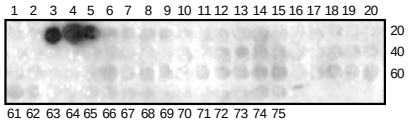

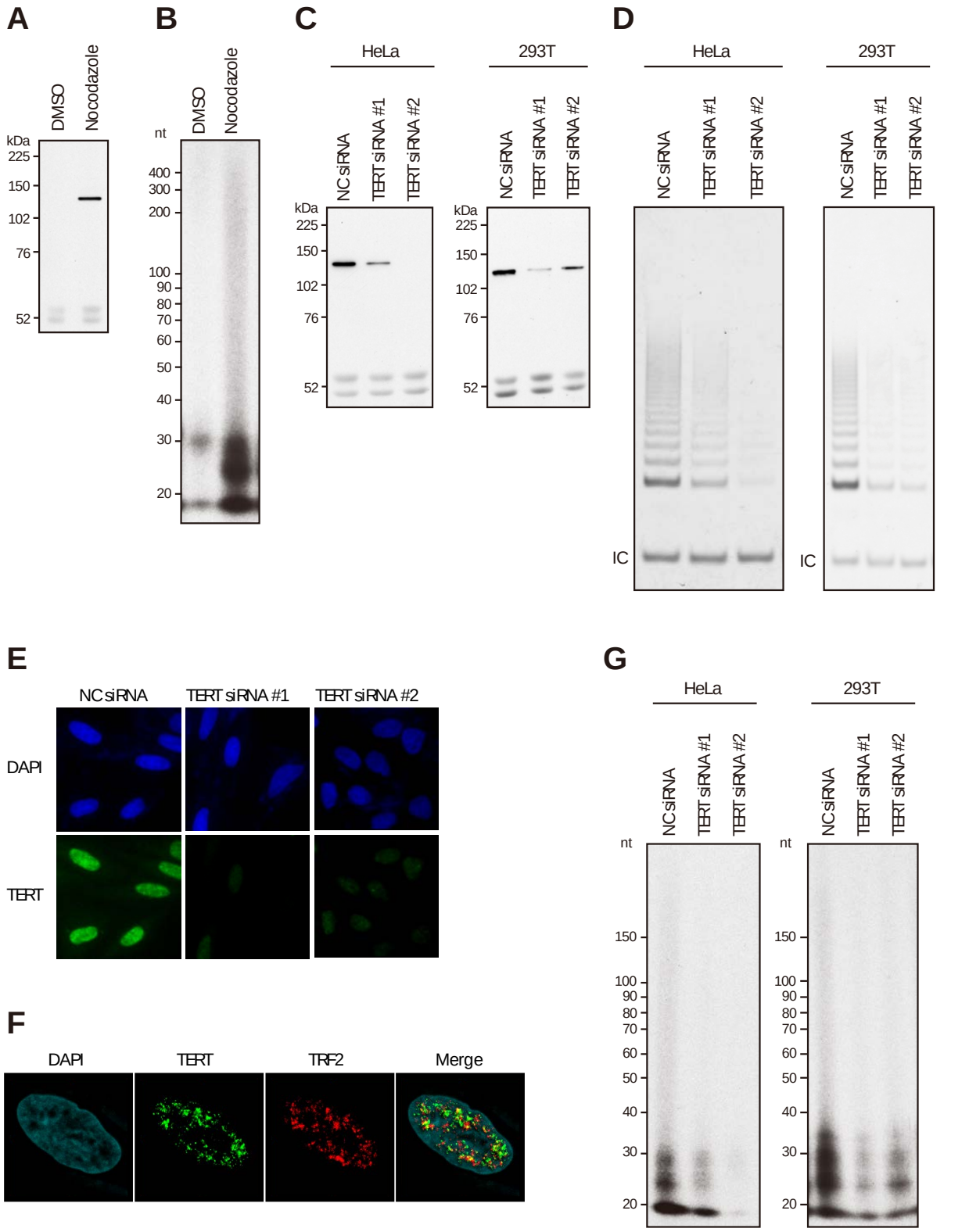

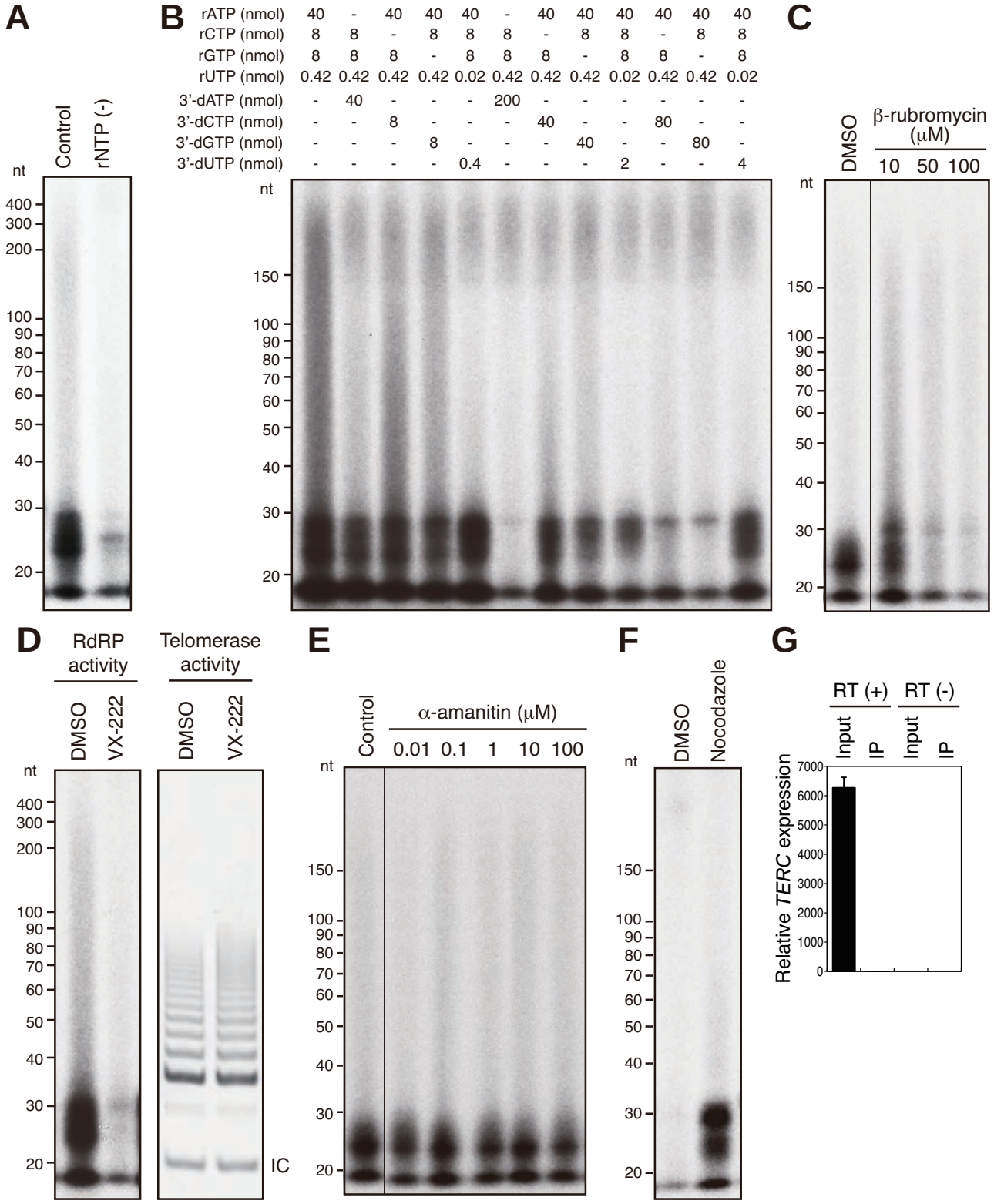

Maida Y, *et al*._Figure 4

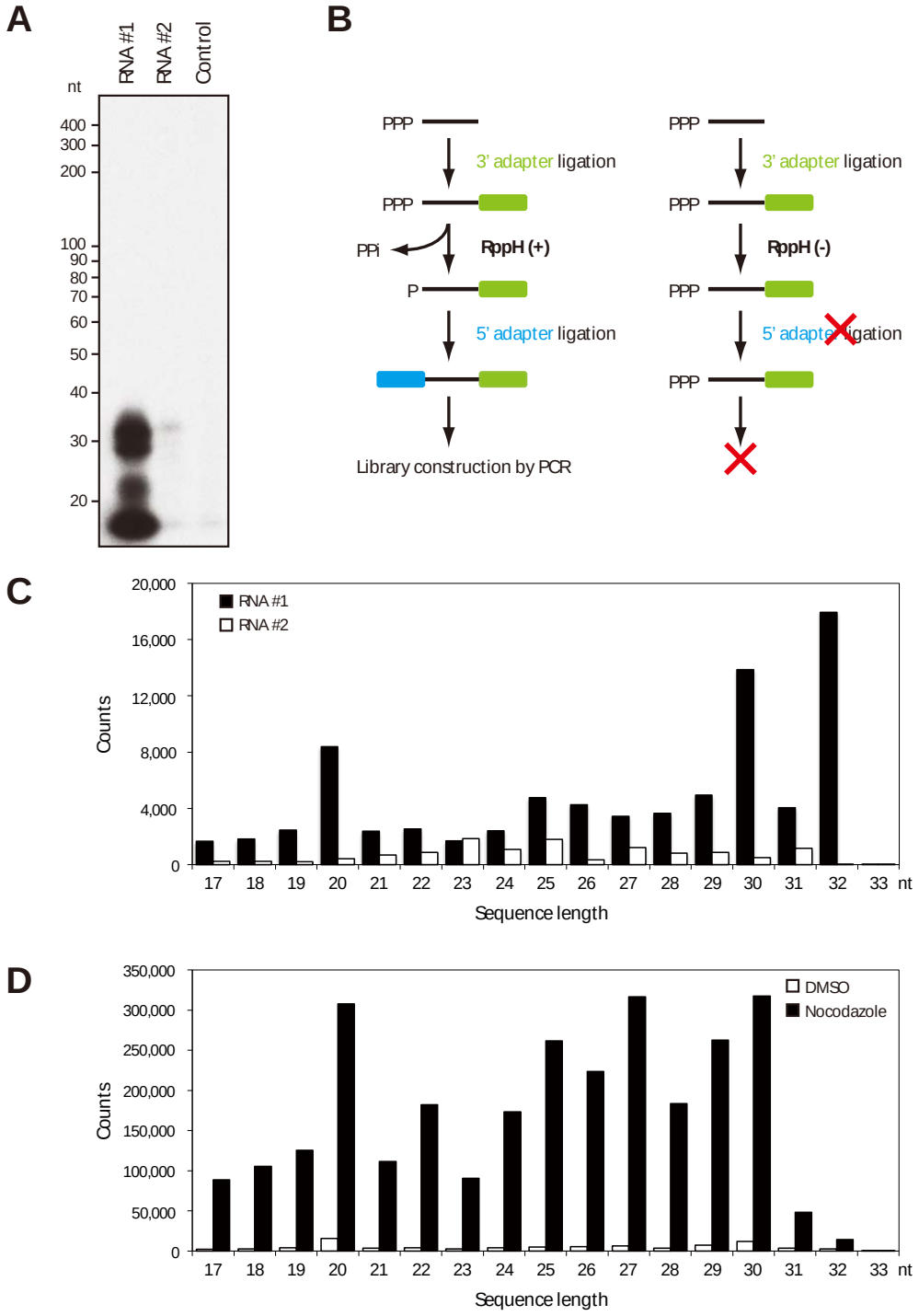

Maida Y, *et al*._Figure 5

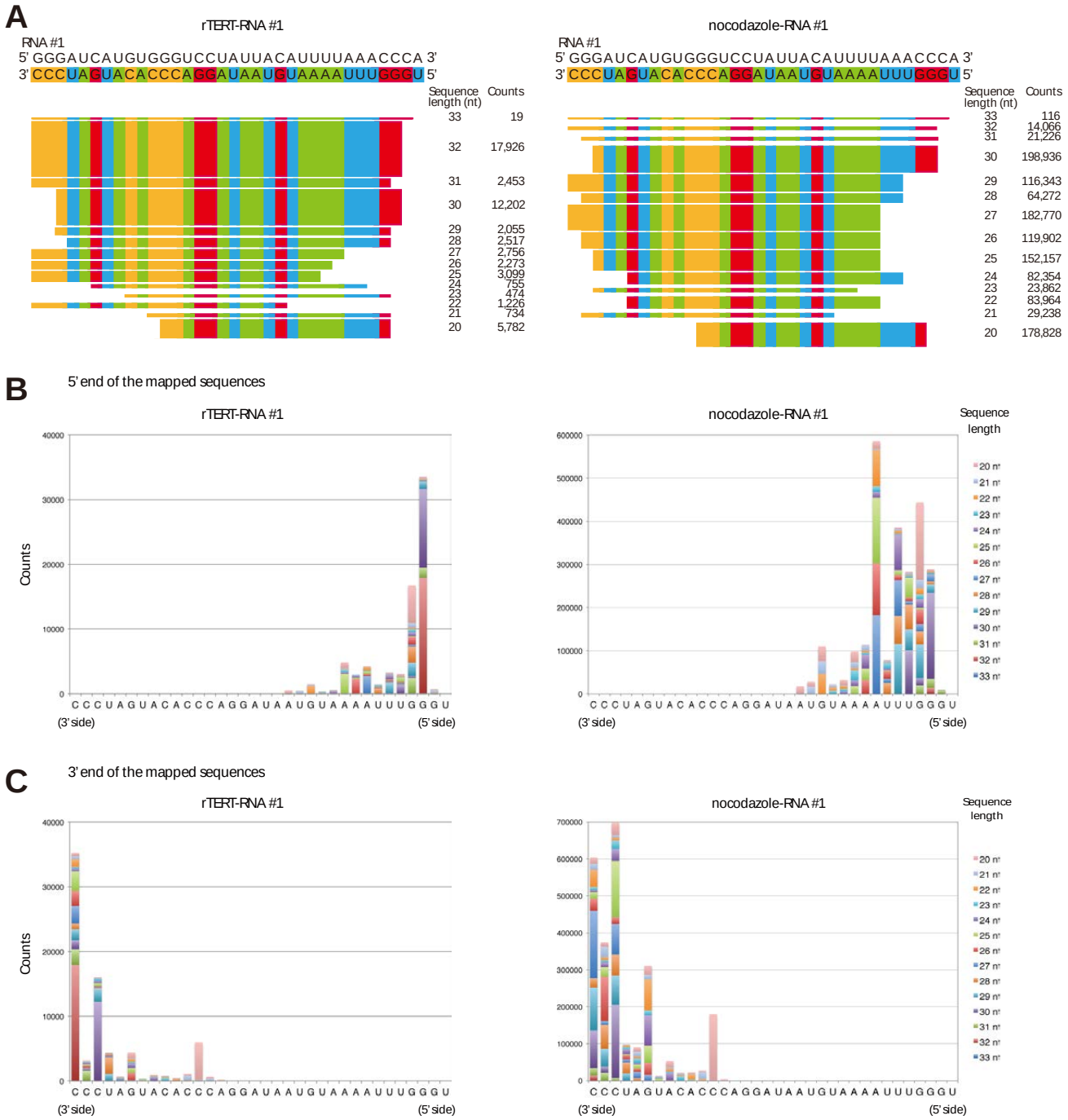

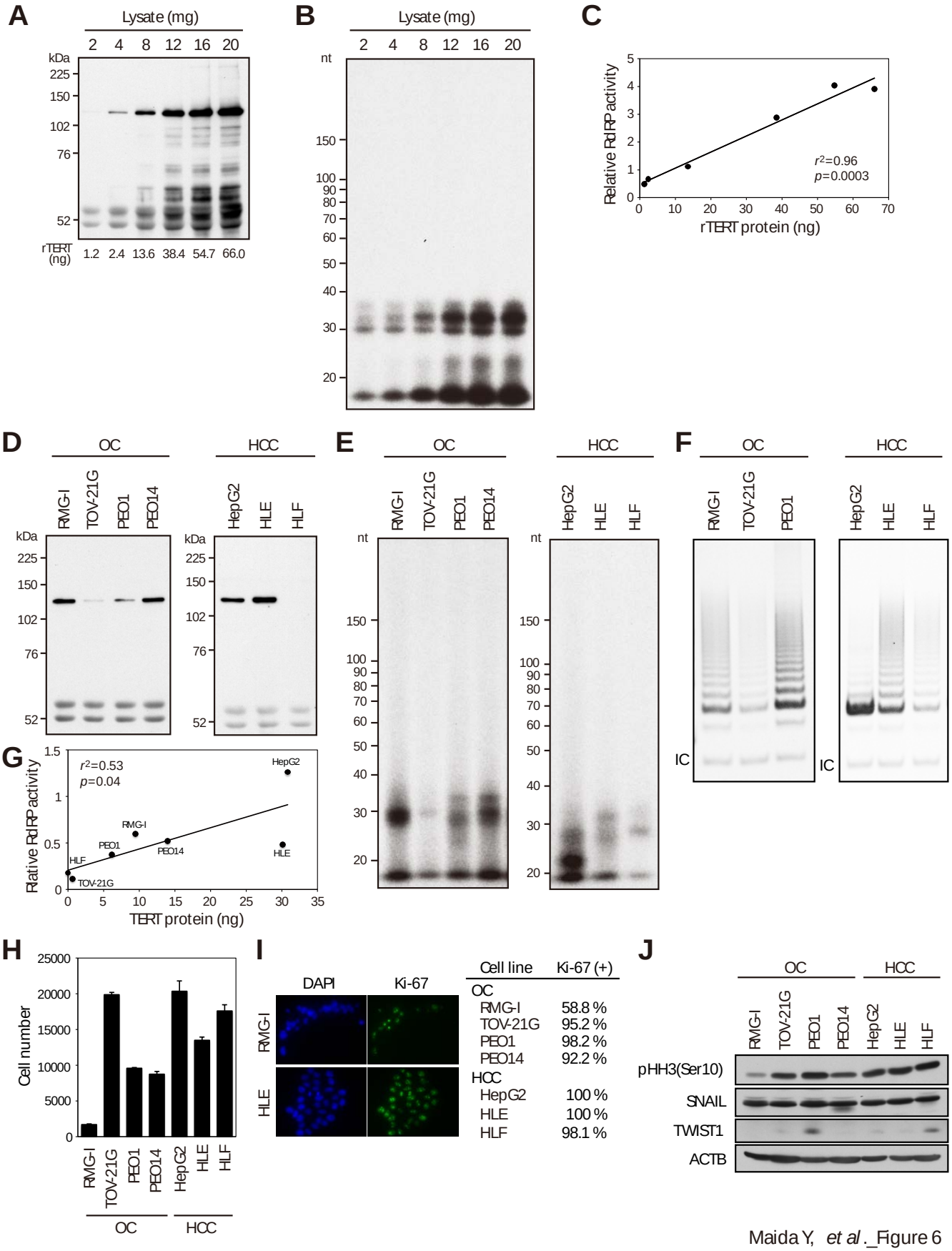

Maida Y, *et al*._Figure 6